

## Electronic stopping of low-energy H and He in Cu and Au investigated by time-of-flight low-energy ion scattering

S. N. Markin, D. Primetzhofer, M. Spitz, and P. Bauer

*Institut fuer Experimentalphysik, Abt. Atom- und Oberflaechenphysik, Johannes Kepler Universitaet, Altenbergerstr. 69, A-4040 Linz, Austria*

(Received 3 June 2009; revised manuscript received 2 October 2009; published 4 November 2009)

Electronic stopping has been investigated experimentally for slow  $H^+$  and  $He^+$  ions ( $v < 0.6$  a.u.) in polycrystalline Au and Cu, by means of time-of-flight low-energy ion scattering. Measurements were performed in backscattering geometry using polycrystalline films of several nanometers thickness; high-resolution Rutherford backscattering spectrometry was used for precise thickness calibration ( $< 4\%$ ). Absolute stopping cross-section data for Cu and Au were obtained down to  $v \sim 0.07$  a.u. Both Au and Cu exhibit a rather sharp, distinctive threshold velocity of  $\sim 0.18$  a.u. for excitation of  $d$  electrons by  $H^+$  and  $He^+$ . Below this threshold, projectiles interact exclusively with  $s$  electrons.

DOI: [10.1103/PhysRevB.80.205105](https://doi.org/10.1103/PhysRevB.80.205105)

PACS number(s): 79.20.Rf, 34.50.Fa, 34.50.Bw

### I. INTRODUCTION

The study of ion propagation in solids is an active field of fundamental science and represents a key quantity for manifold technological applications. A specific interest is addressed to the study of electronic interaction of slow ions with noble metals, e.g., electronic stopping. This topic is still not well understood, as is reflected by substantial discrepancies between theoretical models and experimental results in the range of low ion energies. Better understanding of the underlying physics may support further development of analytical techniques, e.g., low-energy ion scattering (LEIS) for quantitative surface analysis.

Energy loss of a point charge in a free-electron gas (FEG) is expected to be proportional to the ion velocity, if the ion moves with a velocity  $v$  smaller than the Fermi velocity ( $v < v_F$ ).<sup>1-5</sup> This is based on the assumption that excitation of electron-hole pairs from the valence/conduction band occurs via binary collisions of ions with an electron in a FEG. Contributions from core levels are suppressed by a too low value of the maximum energy transfer in this velocity range. Thus, the stopping power  $S = -dE/dx$  in a free-electron gas reads<sup>6-8</sup>

$$S = Q(Z_1, r_s) \cdot v, \quad (1)$$

where the friction coefficient  $Q$  depends on the atomic charge of the projectile,  $Z_1$ , and on the density parameter,  $r_s$ , which is related to the electron density  $n_e$  via  $4\pi r_s^3/3 = 1/n_e$ . The electronic stopping cross section,  $\varepsilon$ , is closely related to  $S$ , via  $\varepsilon = S/n$ , with the atomic density of the target,  $n$ .

Experimental investigations of the energy loss of slow ions in metallic targets in transmission<sup>8-10</sup> and in backscattering<sup>11</sup> geometries discovered a pronounced deviation from velocity proportionality as expected from Eq. (1). These studies revealed that in transition metals a velocity threshold  $v_{th}$  exists for the excitation of  $d$  electrons, which contribute to electronic stopping only for ion velocities  $v > v_{th}$ .

### II. EXPERIMENT

The energy-loss experiments were performed in the time-of-flight (TOF) setup ACOLISSA.<sup>12</sup> In the setup, a beam of

monoenergetic ions is created in an ion source. It passes through an electrostatic chopper and a system of focusing einzel lenses and is directed onto the target at a small angle  $\alpha$ , measured with respect to the surface normal. Projectiles, backscattered by a large angle  $\theta$  (fixed to  $129^\circ$ ) are detected by use of a set of two channel plates in chevron configuration. The recorded time-of-flight spectrum can be subsequently converted to an energy spectrum by a standard procedure.

Two gold and two copper samples were produced in a high-vacuum evaporation system with a base pressure in the  $10^{-8}$  mbar range. As substrate, both, a Si-implanted sputter cleaned Si sample and a commercial Si wafer were used. The Si implantation was performed to amorphize the Si substrate in order to get rid of channeling effects in Rutherford backscattering spectrometry (RBS). During evaporation, the thickness of the evaporated Au and Cu layers was controlled online by a Quartz microbalance. Large distance to the crucible warrants very homogeneous thickness of the evaporated layers. Relatively high evaporation rates ( $> 10$  ML/s) prevented diffusion of Cu into Si. After evaporation, one set of samples (Cu/Au on the Si wafer) was transferred to the TOF-LEIS chamber for subsequent stopping measurements and the second set to the RBS chamber for thickness determination.

In the RBS setup, a high-resolution surface-barrier detector<sup>13-15</sup> permits quantitative thin-film analysis<sup>16,17</sup> with a depth resolution of  $< 2$  nm for Au at an angle of incidence of  $60^\circ$ . For the target films, the thickness was chosen on the one hand to be considerably larger than the RBS depth resolution and on the other hand to yield TOF-LEIS spectra corresponding to a thin film. RBS experiments were performed at the stopping maximum using deuterons with a primary energy of  $\sim 200$  keV.<sup>18</sup> The thickness was evaluated from the width of the RBS spectra by means of simulating software SIMNRA,<sup>19</sup> resulting in  $146 \pm 6$  Å and  $153 \pm 6$  Å for Au and Cu, respectively. The main contributions to this statistical uncertainty are due to channel width (1–2 %), energy calibration of the multichannel analyzer (1–2 %), the angle of incidence ( $\pm 0.5^\circ$ ) and the  $\varepsilon$  values used in the analysis,<sup>18</sup> with a claimed statistical error of  $\pm 3\%$ . The ab-

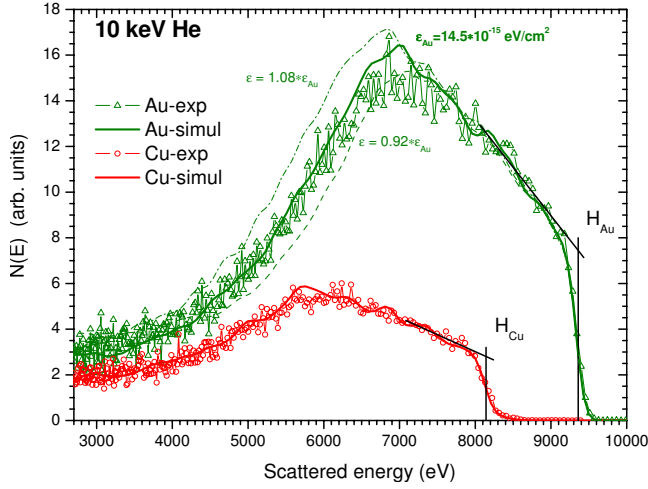


FIG. 1. (Color online) Experimental TOF-LEIS spectra of 10 keV  $\text{He}^+$  ions measured on Cu and Au samples. Also shown the results of TRBS simulations: as solid lines—spectra with optimized  $\varepsilon$ ; as dashed and dashed-dotted lines—spectra with 8% reduced and 8% increased  $\varepsilon$ , respectively.

solute values of these  $\varepsilon$  data are in perfect agreement with the PSTAR recommendation.<sup>20</sup> Nevertheless, any incorrectness of the  $\varepsilon$  values would lead to a systematic error in the deduced thickness, which might exceed the statistical error.

For the relative measurements of  $\varepsilon$ , Cu and Au targets were sputter cleaned by 3 keV  $\text{Ar}^+$ . This was of special importance for the Cu samples, which accumulate surface contaminations more rapidly than Au, which leads to a marked change in the spectrum shape: the high energy onset is blurred, which in relative measurements impedes the evaluation of the spectrum height. The purity of the surface was checked by Auger electron-spectroscopy.

Absolute values of  $\varepsilon$  were obtained from direct comparison of experimental energy spectra with TRBS simulations.<sup>21</sup> TRBS is a Monte Carlo code accounting for multiple scattering, which strongly influences the spectrum shape in LEIS. As projectiles,  $^4\text{He}^+$ ,  $D^+$  and  $D_2^+$  were used, with incident energies in the range 8–10 keV. Since the thickness of the targets was well known, the only free parameter in the simulation was  $\varepsilon$ , which was used to fit the experimental spectrum (see Fig. 1). In the simulations, the ion-atom interaction was described by the Thomas-Fermi-Molière (TFM) potential,<sup>22</sup> with a modified Firsov screening length,  $a_F$ .<sup>23</sup> The choice of the TFM potential was based on the fact that in an independent study the screening length correction for He ions and Cu was determined, resulting in a reduction factor of 0.75.<sup>24</sup> In other cases, the screening length correction is much smaller and O'Connor's recommendations were exploited.<sup>25</sup> TRBS simulations performed using the universal potential did not exhibit any significant changes in the spectrum widths. Thus, for Au, the absolute  $\varepsilon$  derived as described above served as a reference to rescale previous energy-loss measurements<sup>10,26</sup> in order to end up with absolute stopping data for H and He ions in a wider range (see Fig. 2).

In the energy range 0.7–10 keV relative measurements yielded  $\varepsilon$  of H and He ions in Cu ( $\varepsilon_{\text{Cu}}$ ) from an evaluation of the ratio of the experimental spectrum heights,  $H_{\text{Au}}/H_{\text{Cu}}$ ,

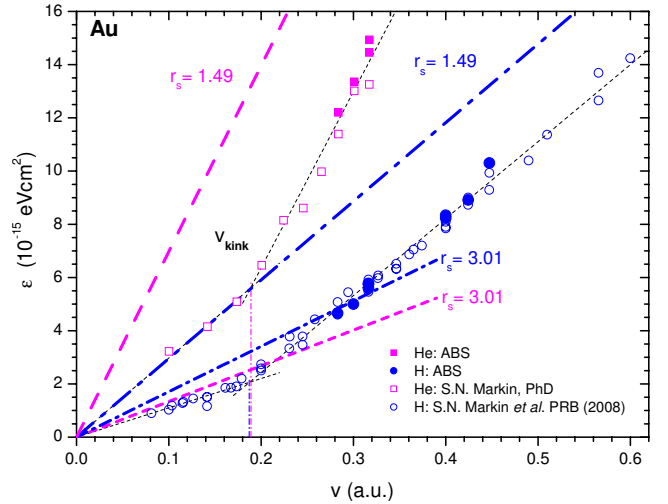


FIG. 2. (Color online) Electronic stopping cross section of H and He ions in Au obtained via absolute measurements (see experiment). Also shown is the data from Refs. 10 and 24. Dash-dotted and dashed lines represent DFT predictions for different density parameters  $r_s$  based on (Refs. 4 and 5) for H and He, respectively.

(see Fig. 1). Within the single-scattering approximation of backscattering spectrometry,<sup>27</sup> the following relation holds

$$\varepsilon_{\text{Cu}} = \varepsilon_{\text{Au}} \cdot \frac{H_{\text{Au}} \cdot \varepsilon_{\text{Au}} \cdot \frac{d\sigma}{d\Omega_{\text{Cu}}}}{H_{\text{Cu}} \cdot \varepsilon_{\text{Cu}} \cdot \frac{d\sigma}{d\Omega_{\text{Au}}}}, \quad (2)$$

where  $d\sigma/d\Omega$  is the differential scattering cross section, calculated for the TFM potential and corrected Firsov screening length;  $\varepsilon$  is the energy per channel. There are two possibilities to extract  $\varepsilon$  from the spectrum heights: either directly from the spectrum heights via Eq. (2) or by use of Monte Carlo simulations. For H ions, both procedures are easily applicable and yield concordant results; spectrum height determination is straightforward due to the unstructured shape of the plateau and the influence of multiple scattering vanishes at the surface. For He ions, the spectrum exhibits a marked surface peak for target materials with a kinematic factor small compared to unity,<sup>28</sup> which hampers a direct evaluation of  $\varepsilon$ . Therefore, in this case the analysis was done exclusively via simulations.

Note, that the number of incident ions in both measurements (Cu and Au) should be identical. A direct measurement is hampered by the extremely low value of the pulsed beam current. Therefore, it is more reasonable to rely on the stability of the primary current. In our case, the beam current was stable within  $\pm 10\%$  and was controlled continuously by repetitive measurements of the count rate of projectiles backscattered from Cu.

### III. RESULTS AND DISCUSSION

Figure 2 presents the experimental electronic stopping cross-section values for H and He ions in Au, as a function of projectile velocity  $v$ . For both projectiles, velocity propor-

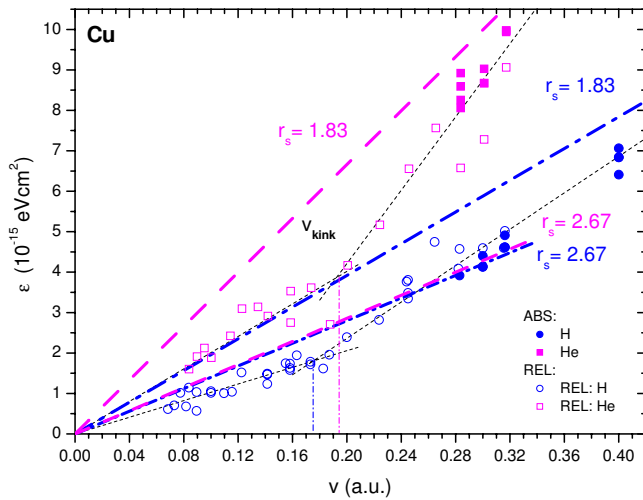


FIG. 3. (Color online) Electronic stopping cross section of H and He ions in Cu obtained via absolute and relative measurements (see experiment). Dash-dotted and dashed lines represent DFT predictions for different density parameters  $r_s$  based on (Refs. 4 and 5) for H and He, respectively.

tional stopping is observed for  $v < 0.19$  a.u., corresponding to 900 eV protons. Above the kink velocity,  $v_{\text{kink}} \approx 0.19$  a.u.,  $5d$  electrons can be excited. Below, incident ions interact exclusively with  $6s$  electrons, which are well described by a FEG. Therefore, velocity proportional stopping is expected.

In Fig. 3,  $\varepsilon$  is plotted for H and He in Cu. The absolute values are depicted as full symbols. The open symbols represent the relative data deduced from the Au stopping by evaluation of the spectrum heights using Eq. (2). Both procedures yield coincident sets of  $\varepsilon$  data for both, H and He ions. This gives very much confidence in the methods applied since otherwise systematic discrepancies should be visible.

As for Au, two regimes are observed for  $\varepsilon$  of H and He in Cu: first, at  $v < 0.17$  a.u. for H ( $v < 0.19$  for He),  $\varepsilon$  is proportional to the ion velocity. There, the projectiles interact only with Cu  $4s$  electrons. Second, at velocities above these kink velocities,  $3d$  electrons take part in the electronic stopping process. In consequence, this leads to a steeper slope of  $\varepsilon(v)$ . The kink velocity for the interaction of projectiles with Cu  $3d$  electrons is almost equal to that of Au. This can be related to the fact that the density of states is very similar for Cu and for Au.<sup>29</sup> The scatter of relative data (open symbols) in Fig. 3 is due to fluctuations in the incident-beam current, leading to a statistical uncertainty of less than  $\pm 15\%$  per data point.

The electronic stopping of both, H and He in Au is systematically higher than in Cu. This is a matter of fact and not yet well understood. For Au, the density parameter,  $r_s$ , is  $\sim 13\%$  higher than for Cu. Therefore, theory would predict a smaller  $\varepsilon$  for Au,<sup>5</sup> in contrast to experimental observation.

In Figs. 2 and 3, also theoretical results are depicted, based on density-functional theory (DFT).<sup>4,5</sup> DFT provides  $r_s$ -dependent friction coefficients for H and He projectiles,  $Q(Z_1, r_s)$ , according to Eq. (1). For H ions, two sets of lines are shown for both, Au and Cu. The short dash-dotted blue

(black) lines at  $v < 0.3$  refer to the DFT results for the limiting case of only one electron participating in the stopping process, corresponding to  $r_s = 2.67$  and  $3.01$  for Cu and Au, respectively. In both cases, good agreement is obtained with an overestimation of the experimental data by  $\sim 20\text{--}30\%$ . Note that these predictions should be realistic only if the  $d$  electrons would neither participate in screening nor in the interaction with the screened ion charge.

The dash-dotted blue (black) lines refer to the case when all conduction electrons participate in the interaction, with effective  $r_s$  values of  $1.83$  and  $1.49$  for Cu and Au, respectively, as deduced from experimental plasmon energies.<sup>5,30</sup> Note that in the experiment only for velocities  $v > 0.6$  a.u. all conduction electrons ( $s$ ,  $p$ , and  $d$  electrons) can be excited. Thus, the stopping cross sections corresponding to these  $r_s$  values are not expected to be directly applicable in the presented velocity regime. For Au, the DFT result exhibits virtually the same slope as the experimental data. Thus, the theoretical values are expected to overestimate  $\varepsilon$  in the whole range  $v < v_F = 1.92/r_s$ . For Cu, the situation is similar but the overestimation of the data by the DFT result is far less pronounced; very good agreement is expected for velocities  $v > 0.6$ .

As one can see in Figs. 2 and 3, for He, the experimental stopping cross-section data are much higher than that for H in the whole velocity range investigated. This is in contrast to the DFT results for the energy loss in a diluted FEG, represented by the magenta (gray) short dashed lines, that correspond to  $r_s = 2.67$  and  $3.01$  for Cu and Au, respectively. One of the predictions of DFT is that in a dilute electron gas with  $r_s > 2.7$ , electronic stopping of He ions is less effective than for H ions, as is evident in Figs. 2 and 3 from the comparison of full and dashed lines. There is, however, a major difference between the situation described by theory and the real physical properties of our target material: in Au, the projectile charge will be screened at all ion velocities collectively by  $5d$  and  $6s$  electrons, which act as a high-density electron gas, while electron-hole pairs can be excited only from the low-density  $6s$  band, when the ion velocity is smaller than  $0.19$  a.u. Note that recent experiments performed in transmission of slow H and He ions through a Au(100) single crystal in channeling geometry<sup>9</sup> exhibited a decreasing  $\varepsilon$  ratio  $\varepsilon_{\text{He}}/\varepsilon_{\text{H}}$  with decreasing velocity until it reaches unity at  $v \approx 0.14$  a.u., as predicted by DFT. This may be taken as indication that the interaction distance is of major importance as discussed below.

The DFT results corresponding to the interaction with all conduction electrons [magenta (gray) dashed lines in Figs. 2 and 3], are similar to those for H ions: for Au, theory is expected to overestimate the experimental data in the range  $v < v_F$  while for Cu the DFT results are much closer to experimental values.

The comparison of electronic-energy loss in a backscattering experiment and in a transmission measurement in channeling through a single crystal deserves further discussion. On the one hand, in a transmission channeling experiment, ions cannot experience close collisions with target atoms. This leads to minimum electronic-energy loss for perfect channeling and an increase by  $< 10\%$  for exit angles up to  $8^\circ$ .<sup>31</sup> On the other hand, also in backscattering not all inter-

action distances contribute to the electronic interaction, since especially for close collisions and low energies the minimum distance in a collision with an atom is much larger than the impact parameter. Consequently, one has to consider the possibility that the friction coefficient  $Q$  exhibits an energy dependence since very slow ions do not come close to the ion cores and thus cannot explore the high electron density there.<sup>32,33</sup>

For Au(100), e.g., in channeling the effective electron density is known to correspond to  $r_s=1.8$ ; this value is very close to the  $r_s$  value for polycrystalline Cu.<sup>34</sup> The present results for Cu are in good agreement with this finding: for  $v > 0.2$  a.u. the ratio  $\varepsilon_{\text{He}}/\varepsilon_{\text{H}}$  deduced from the data shown in Fig. 3 is very much consistent with the energy-loss ratios  $\Delta E_{\text{He}}/\Delta E_{\text{H}}$  for Au(100) evaluated from the data presented in Ref. 10.

In summary, we investigated electronic stopping of H and He ions in polycrystalline Au and Cu in the regime of very low ion velocities. Measurements were performed in backscattering geometry by means of TOF-LEIS. We obtained

absolute stopping cross-section values with an uncertainty  $< \pm 0.5 \times 10^{-15}$  eV cm<sup>2</sup> per data point. For both materials we observed a clear threshold for the excitation of  $d$  electrons at  $v \approx 0.18\text{--}0.19$  a.u.; below this threshold the projectiles interact exclusively with the  $s$  electrons. While DFT predicts  $\varepsilon_{\text{He}} < \varepsilon_{\text{H}}$ , when in a free-electron gas the number of interacting electrons is reduced, our experimental values do not exhibit any statistically significant velocity dependence. From this we conclude that in the materials investigated the existence of an excitation threshold for  $d$  electrons cannot be mimicked by a transition from a high density to a low-density electron gas.

#### ACKNOWLEDGMENTS

This work has been supported by Austrian FWF (Projects No. 17449-N02 and No. P19595-N20). D.P. acknowledges financial support by the Austrian Academy of Science. Inspiring discussions with Inaki Juaristi, Andres Arnau, and Istvan Nagy are gratefully acknowledged.

- 
- <sup>1</sup>J. Lindhard, K. Dan. Vidensk. Selsk. Mat. Fys. Medd. **28**, 1 (1954).
- <sup>2</sup>T. L. Ferrell and R. H. Ritchie, Phys. Rev. B **16**, 115 (1977).
- <sup>3</sup>A. Mann and W. Brandt, Phys. Rev. B **24**, 4999 (1981).
- <sup>4</sup>P. M. Echenique, R. M. Nieminen, and R. H. Ritchie, Solid State Commun. **37**, 779 (1981).
- <sup>5</sup>I. Nagy, A. Arnau, and P. M. Echenique, Phys. Rev. A **40**, 987 (1989).
- <sup>6</sup>P. M. Echenique, F. Flores, and R. H. Ritchie, Solid State Phys. **43**, 229 (1990).
- <sup>7</sup>G. Martínez-Tamayo, J. C. Eckardt, G. H. Lantschner, and N. R. Arista, Phys. Rev. A **54**, 3131 (1996).
- <sup>8</sup>J. E. Valdés, J. C. Eckardt, G. H. Lantschner, and N. R. Arista, Phys. Rev. A **49**, 1083 (1994).
- <sup>9</sup>E. A. Figueroa, E. D. Cantero, J. C. Eckardt, G. H. Lantschner, J. E. Valdés, and N. R. Arista, Phys. Rev. A **75**, 010901 (2007).
- <sup>10</sup>C. Celedón, N. R. Arista, J. E. Valdés, and P. Vargas, Microelectron. J. **39**, 1358 (2008).
- <sup>11</sup>S. N. Markin, D. Primetzhofer, S. Prusa, M. Brunmayr, G. Kowarik, F. Aumayr, and P. Bauer, Phys. Rev. B **78**, 195122 (2008).
- <sup>12</sup>M. Draxler, S. N. Markin, S. N. Ermolov, K. Schmid, C. Hesch, R. Gruber, A. Poschacher, M. Bergsmann, and P. Bauer, Vacuum **73**, 39 (2004).
- <sup>13</sup>M. Geretschlager, Nucl. Instrum. Methods **204**, 479 (1983).
- <sup>14</sup>P. Bauer and G. Bortels, Nucl. Instrum. Methods Phys. Res. A **299**, 205 (1990).
- <sup>15</sup>E. Steinbauer, G. Bortels, P. Bauer, J. P. Biersack, P. Burger, and I. Ahmad, Nucl. Instrum. Methods Phys. Res. A **339**, 102 (1994).
- <sup>16</sup>P. Bauer, Nucl. Instrum. Methods Phys. Res. B **27**, 301 (1987).
- <sup>17</sup>P. Mertens and P. Bauer, Nucl. Instrum. Methods Phys. Res. B **33**, 133 (1988).
- <sup>18</sup>D. Semrad, P. Mertens, and P. Bauer, Nucl. Instrum. Methods Phys. Res. B **15**, 86 (1986).
- <sup>19</sup>M. Mayer, Nucl. Instrum. Methods Phys. Res. B **194**, 177 (2002).
- <sup>20</sup>M. J. Berger, J. S. Coursey, and M. A. Zucker, ESTAR, PSTAR, and ASTAR: *Computer Programs for Calculating Stopping-Power and Range Tables for Electrons, Protons, and Helium Ions*, Version 1.2.2. National Institute of Standards and Technology, Gaithersburg, MD, 2000 (<http://physics.nist.gov/Star>).
- <sup>21</sup>J. P. Biersack, E. Steinbauer, and P. Bauer, Nucl. Instrum. Methods Phys. Res. B **61**, 77 (1991).
- <sup>22</sup>G. Moliere, Z. Naturforsch. A **2a**, 133 (1947).
- <sup>23</sup>O. B. Firsov, Sov. Phys. JETP **6**, 534 (1958).
- <sup>24</sup>D. Primetzhofer, S. N. Markin, M. Draxler, R. Beikler, E. Taglauer, and P. Bauer, Surf. Sci. **602**, 2921 (2008).
- <sup>25</sup>D. J. O'Connor and J. P. Biersack, Nucl. Instrum. Methods Phys. Res. B **15**, 14 (1986).
- <sup>26</sup>S. N. Markin, Ph.D. thesis, J. K. University Linz, 2007.
- <sup>27</sup>W. K. Chu, J. W. Mayer, and M. A. Nicolet, *Backscattering Spectrometry* (Academic, New York, 1978), Chap. 3.
- <sup>28</sup>M. Draxler, R. Beikler, E. Taglauer, K. Schmid, R. Gruber, S. Ermolov, and P. Bauer, Phys. Rev. A **68**, 022901 (2003).
- <sup>29</sup>C. J. Fall, N. Bingelli, and A. Baldereschi, Phys. Rev. B **61**, 8489 (2000).
- <sup>30</sup>H. R  ther, *Excitation of Plasmons and Interband Transitions by Electrons* (Springer, Berlin, 1980).
- <sup>31</sup>E. A. Figueroa, E. D. Cantero, J. C. Eckardt, G. H. Lantschner, M. L. Martiarena, and N. R. Arista, Phys. Rev. A **78**, 032901 (2008).
- <sup>32</sup>P. L. Grande and G. Schiwietz, Phys. Lett. A **163**, 439 (1992).
- <sup>33</sup>G. Schiwietz and P. L. Grande, Nucl. Instrum. Methods Phys. Res. B **90**, 10 (1994).
- <sup>34</sup>J. E. Valdés, P. Vargas, C. D. Denton, and N. R. Arista, Nucl. Instrum. Methods Phys. Res. B **193**, 43 (2002).